Available online at www.sciencedirect.com
ScienceDirect
Vision Research 47 (2007) 1394–1409
Vision Research
www.elsevier.com/locate/visres

Form vision in the insect dorsal ocelli: An anatomical and optical analysis of the dragonfly median ocellus

Richard P. Berry [a,*], Gert Stange [a], Eric J. Warrant [b]

[a] Centre for Visual Sciences, Research School of Biological Sciences, Australian National University, Canberra, Australia
[b] Department of Cell and Organism Biology, University of Lund, Lund, Sweden

Received 2 November 2006; received in revised form 16 January 2007

Abstract

Previous work has suggested that dragonfly ocelli are specifically adapted to resolve horizontally extended features of the world, such as the horizon. We investigate the optical and anatomical properties of the median ocellus of *Hemicordulia tau* and *Aeshna mixta* to determine the extent to which the findings support this conclusion. Dragonfly median ocelli are shown to possess a number of remarkable properties: astigmatism arising from the elliptical shape of the lens is cancelled by the bilobed shape of the inner lens surface, interference microscopy reveals complex gradients of refractive index within the lens, the morphology of the retina results in zones of high acuity, and the eye has an exceedingly high sensitivity for a diurnal terrestrial invertebrate. It is concluded that dragonfly ocelli employ a number of simple, yet elegant, anatomical and optical strategies to ensure high sensitivity, fast transduction speed, wide fields of views and a modicum of spatial resolving power.

Keywords: Insect; Ocelli; Optics; Acuity; Modelling

1. Introduction

Among insects, both the median and lateral ocelli of dragonflies show a number of unique properties which suggest that their function is unlike those of other ocelli. In particular, dragonfly ocelli do not appear to function as underfocused wide field illumination detectors or 'single sensors' (Stange, Stowe, Chahl, & Massaro, 2002), as has been suggested to be the major function of other ocelli (Wilson, 1978).

Earlier work on the dioptrics and anatomy of the dragonfly median ocellus (Stange et al., 2002) first suggested that this eye may be specifically adapted to resolve horizontally extended features of the world. In particular, the median ocellar lens is strongly elliptical, with the long axis horizontal. The outer lens surface is strongly curved, but in an anisotropic manner such that the radius of curvature is smaller in the vertical plane than in the horizontal plane. The shape of the lens surface suggests that the image formed is astigmatic, but that vertically modulated features are focused within the retina. Stange et al. (2002) were able to partially verify this by observing the image formed by the lens of a point source of light. Close to the rear surface of the lens (presumed to be the vertical focal plane), the image formed was a well defined horizontal streak. Proximal to this, another image was formed which was approximately circular, but less well defined in all directions. These results supported the predictions from the anatomy of the eye, and showed that at least one of the two foci formed by the lens does not lie beyond the proximal limit of the retina. This was further supported by observations of tapetal reflections from the eye, which showed that the visual field is wide and elliptical, and that the resolving power of the optics is a factor of two better in the vertical plane than in the

* Corresponding author. Address: Research School of Biological Sciences, Australian National University, P.O. Box 475, Canberra, ACT 2601, Australia. Fax: +61 2 61253808.
E-mail address: rberry@rsbs.anu.edu.au (R.P. Berry).

0042-6989/$ - see front matter © 2007 Elsevier Ltd. All rights reserved.
doi:10.1016/j.visres.2007.01.019

horizontal plane. Lastly, ultrastructural analysis of the retina revealed the rhabdoms to be partially sheathed by reflecting tapetum. Optical isolation of rhabdoms is known to improve both sensitivity and spatial resolution, especially in eyes of low *F*-number (Warrant & McIntyre, 1991).

More direct evidence for the preservation of spatial information is obtained from electrophysiological analysis of ocellar photoreceptors. van Kleef, James, and Stange (2005) describe the median ocellar photoreceptors as having elliptical receptive fields, with acceptance angles in azimuth twice as wide as those in elevation. A similar analysis of the large second order neurons (L-neurons) shows that spatial information is retained after convergence from photoreceptors to second-order neurons. L-neurons of both the median (Berry, Stange, Olberg, & van Kleef, 2006), and lateral (Berry, van Kleef, & Stange, 2007a) ocelli form a one-dimensional spatial map of the environment that is extended in azimuth, but restricted in elevation.

Further support for the unique nature of the dragonfly ocelli is given by the finding that directionally selective responses are mediated through these eyes. Zenkin and Pigarev (1971) recorded extracellular responses of units in the ventral nerve cord of several species of dragonfly which responded to the upwards and downwards motion of gratings in a directionally selective manner. Little to no directionally selective responses could be elicited by the movement of vertical bars to the left or right. These responses could be attributed to stimulation of the ocelli alone, as they were abolished upon occlusion of the ocelli, but not the compound eyes. These findings support the conclusions drawn from analysis of the median ocellus by Stange et al. (2002); namely that this eye is adapted to detect horizontally extended features of the world.

One objective of the present paper is to determine the extent to which the morphology and optics of the median ocellus of dragonflies are consistent with determinations of the spatial transfer characteristics of this sensory system as obtained by other methods. A second objective is to determine the extent to which the structures constituting the retina and synaptic plexus support spatial resolution. Additionally, preliminary investigation of the dioptrics of the median ocellus revealed two peculiarities of the lens, namely that the image formed was bilaterally split, and the short focal length of the lens suggested the presence of refractive index gradients. These features warranted an intensive investigation into the dioptrics and morphology of this eye.

The basic morphology and dioptrics of the dragonfly median ocellus are investigated by standard histological and optical techniques. This is followed by the development of ray tracing models, which allow theoretical angular sensitivity functions of individual photoreceptors to be obtained. Lastly, complex properties of the median ocellar lens are investigated by use of the ray tracing models, as well as by interference microscopy.

2. Methods

2.1. Experimental animals

Two species of dragonfly, *Hemicordulia tau* (Corduliidae) and *Aeshna mixta* (Aeshnidae) were used for optical and morphological analysis. One species of dragonfly, *Sympetrum danae* (Libellulidae) was used for interference microscopy. *Hemicordulia* were either caught locally in the area of Canberra, Australia, or were raised from the larval stage in the laboratory, and used for experimentation within two days of emergence. *Aeshna* and *Sympetrum* were obtained by netting in the area of Lund, Sweden. All dragonflies were stored in the dark at 4 °C until used for experimentation.

2.2. Histology and three-dimensional reconstructions

Light microscopy was performed on *Hemicordulia* and *Aeshna*. Histological procedures used for dragonfly ocelli are identical to those used for locust ocelli as described in the accompanying publication (Berry, Warrant, & Stange, 2007b), with the exception that some samples were embedded in a soft Araldite 502/Epon 812 resin. This allowed the collection of thick (15–30 μm) sections on an AOC Spencer 820 rotary microtome.

Selected sets of serial sections were used to generate three-dimensional reconstructions of the median ocellus of *Hemicordulia*. Reconstruction processes used are identical to those described in the accompanying publication.

2.3. Analysis of dioptrics

Back focal distances (BFDs), focal lengths and imaging quality of excised median ocellar lenses were investigated by use of the hanging drop technique (Homann, 1924). The imaging quality of the lenses of *Hemicordulia* was obtained by measuring the modulation transfer function (MTF) of the lens at various points of defocus behind the inner lens surface, over a range of distances that covers the entire scope of the retina. This procedure is a deviation of the procedure described by Schuppe and Hengstenberg (1993) and has been described in detail in the accompanying publication. Briefly, a microscope objective was initially focused on the inner surface of an ocellar lens inversely suspended in a water droplet. At incrementally increasing distances behind the inner lens surface, a series of images of sinusoidally modulated gratings of various wavelengths was recorded. The contrast of bars in the gratings varied in either the vertical (sagittal) or horizontal (transverse) plane. The contrast present in each of the images was determined and used to construct MTFs at each point of defocus. Spatial cut-off frequencies are determined from each of the MTFs, and described as a function of distance from the inner lens surface.

In the case of *Aeshna*, the imaging quality of the median ocellar lens was determined only at the focal plane of the lens, from gratings of various known spatial wavelengths placed onto the lamp of a microscope. Gratings consisted of square wave light and dark bars ranging in spatial wavelength from 8.81° to 0.22°, and consisting of a 50% duty cycle such that the average intensity of light passing through the grating remained constant. A small error in the resulting MTF of the lens arises from using square wave rather than sinusoidal gratings. This error was considered to be negligible and was not accounted for. Images were acquired manually on a Nikon FE2 35 mm camera using exposure times that resulted in the highest contrast images. Negatives were then digitised by scanning on a Polaroid Sprintscan 35. Greyscale values from the image were obtained and used to determine the contrast present in the image in a manner identical to that described in the accompanying publication.

The focal length (f) of each lens was also directly determined by transverse magnification using the formula:

$$f = s\frac{\lambda_i}{\lambda_o}, \tag{1}$$

where s is the distance between a test object and the lens, λ_o is the size of the object, and λ_i the size of the corresponding image at the focal plane.

2.4. Interference microscopy

The ocellar lenses of two adult *Sympetrum* were used for interference microscopy. The lenses were excised and frozen in a droplet of saline, which in turn was mounted in Tissue-Tek (Electron Microscopy Sciences). Approximately, 14 μm thick sections were cut at −16 °C on a Reichert-Jung cryotome, then mounted and coverslipped in saline (refractive index of 1.34). Sections were observed under a Zeiss interference microscope (Jamin-Lebedeff type). Monochromatic light of 546 nm wavelength was split into a measurement beam, which passed directly through the lens, and a reference beam which passed just to the side of the lens. Recombination of these two beams yielded interference fringes in the lens. Estimations of the refractive index of the central region of the lens were determined by establishing the amount of phase shift required to match the interference colour of the lens to that of the surrounding medium. Selected sections were imaged with a Nikon FE2 35 mm camera.

2.5. Ray tracing

Geometrically accurate models of the median ocellus of *Hemicordulia* were created in Matlab™ (Mathworks). The models consisted of a lens and a rhabdom array, and described the median ocellus in two-dimensional cross-section in either the horizontal or vertical plane. All parameters used to define the geometry of the median ocellus were determined from histological sections.

Ray tracing was achieved by calculating the trajectory of a given ray and determining whether or not this line intersects with any lens or rhabdom structure. Upon intersection with an object, the ray is refracted according to Snell's law:

$$n_1 \sin\theta_1 = n_2 \sin\theta_2, \tag{2}$$

where n_1 and n_2 are the refractive indices on either side of the refractive interface, and θ_1 and θ_2 are the incoming and outgoing angles of the ray with respect to the normal. Where total internal reflection occurs, or where a ray is incident on reflecting tapetum, θ_2 is simply equal to θ_1. Unless otherwise stated, the following refractive indices were assigned; lens: 1.5; medium surrounding outer lens surface: 1; medium surrounding inner lens surface: 1.34; rhabdoms: 1.36. The validity of the ray tracing model was checked by tracing rays through lenses of dimensions for which the focal length can be easily calculated by standard optical formulae (e.g. spherical lenses).

Light rays were given an arbitrary value describing the energy initially contained in the light ray (for simplicity a value of 1 was used). When incident on a rhabdom, a fraction of this energy was absorbed. This was described by:

$$F_{\text{abs}} = (1 - e^{-kx}), \tag{3}$$

where x is the length of rhabdom the ray passes through and k is the absorption coefficient, for which a value of 0.0067 μm^{-1} was taken as typical of arthropod photoreceptors (Land, 1981; Warrant & Nilsson, 1998).

Angular sensitivity functions of rhabdoms were generated by tracing rays through the lens at angles of incidence that increased in 0.5° steps. At each angle of incidence, the total amount of light absorbed by each rhabdom in the array was recorded. Over 120 parallel rays were traced through the lens at each angle of incidence, each ray being offset from its neighbours by 3–4 μm. The validity of the angular sensitivity functions was checked by tracing rays through a spherical lens with a uniformly circular rhabdom layer arranged behind the lens. As expected, this resulted in nearly identical angular sensitivity functions from each of the rhabdoms in the array.

2.6. Theoretical description

Theoretical focal lengths were determined from the radii of curvatures of the inner and outer surfaces of the dragonfly median ocellar lens (as ascertained from histological sections) using the following equation (Land, 1981):

$$\frac{1}{f} = \frac{n_2 - n_1}{r_1} + \frac{n_3 - n_2}{r_2} - \frac{d(n_2 - n_1)(n_3 - n_2)}{n_2 r_1 r_2}, \tag{4}$$

where n_1, n_2 and n_3 are the refractive indices of the outer surrounding medium, the lens, and the inner surrounding medium, respectively, r_1 and r_2 are the radii of curvatures of the inner and outer surfaces of the lens, f is the focal length, and d is the distance separating the two refracting surfaces.

The optical sensitivity (S, in units of μm^2 sr) of an elliptical eye in broad spectrum light (Warrant & Nilsson, 1998) can be calculated from a slightly revised form of the Land sensitivity equation:

$$S = \left(\frac{\pi}{4}\right)^2 AB\left(\frac{d}{f}\right)^2 \left(\frac{kx}{2.3 + kx}\right), \tag{5}$$

where A and B are the dimensions of the lens across its major and minor axes, respectively, f is the focal length, d is the diameter of the rhabdom, x is its length, and k the absorption coefficient.

3. Results

3.1. General orientation

In the dragonfly, the ocelli are located as a triplet on the front of the head (Fig. 1). The median ocellus lies ventral to the lateral ocelli and is recessed into a groove that is bounded ventrally by the frons, and dorsally by the vertex. The field of view of the median ocellus is elongated in the horizontal direction and centred approximately parallel to the long axis of the body (Stange et al., 2002), such that in level flight, this eye is centred on the horizon (elevation and azimuth of 0°).

3.2. Histology of the dragonfly median ocellus

3.2.1. The median ocellar lens

The dimensions and morphology of the dragonfly median ocellus given here conform closely to those described

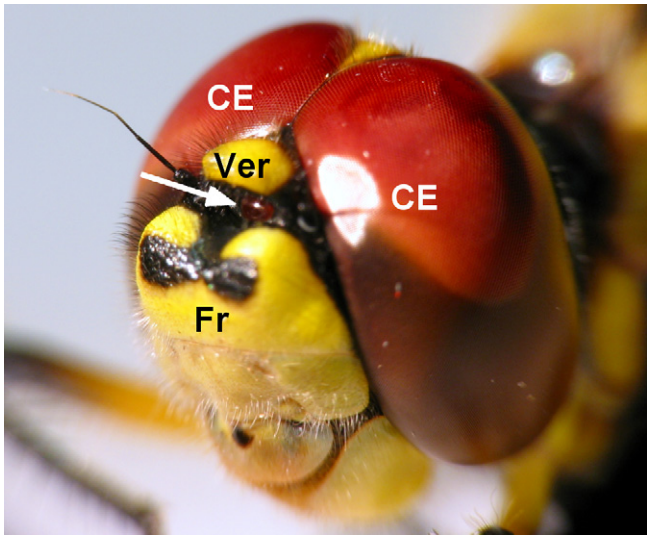

Fig. 1. Photograph of the head of *Hemicordulia tau*. The ocelli are located anterior to the prominent compound eyes (CE). The median ocellus (arrow) is recessed into a groove above the frons (Fr) and below the vertex (Ver). The elevational field of view of the median ocellus is constrained by these structures. In level flight the optical axis of the median ocellus lies approximately parallel with the long body axis of the dragonfly.

previously for *Hemicordulia* (Stange et al., 2002), and for other species of dragonfly (Chappell & Dowling, 1972; Dowling & Chappell, 1972; Rosser, 1974; Ruck & Edwards, 1964; Stange et al., 2002). Therefore only a brief description is given below, with values given in Table 1 where possible.

The median ocellar lens is elliptical, with the long axis in the horizontal direction. The lens of *Aeshna* is larger and more strongly elliptical than that of *Hemicordulia*, with width/height aspect ratios of 1.5 in the former and 1.3 in the latter.

From reconstructions of the lens (Fig. 2), as well as comparison of sections taken in horizontal and vertical orientations through the eye (Fig. 5), it can be seen that the radius of curvature of the outer lens surface differs between the horizontal and vertical planes. In the vertical plane, the radius of curvature is smaller and closely approximates a circle. In the horizontal plane, the radius of curvature is 1.2–1.4 times larger (Table 1) and non-uniform, decreasing toward the periphery of the lens.

Below the level of the cuticle the lens becomes constricted to form an elongated cylinder. The inner surface of the lens is also anisotropic in the vertical and horizontal planes, as also described by Stange et al. (2002). Whereas the external surface of the lens appears as a single, smooth surface, the inner surface is split bilaterally into left and right halves. This is particularly evident in reconstructions of the median ocellus (Fig. 2). Ventrally, a distinct depression is observed running down the midline of the lens which separates the inner surface into distinct left and right lobes. Further dorsally, the inner surface becomes flatter, and the depression dividing the lens into left and right lobes is replaced by a pronounced cuticular ridge protruding outward from the inner surface.

Table 1
Dimensions of the dragonfly median ocellus as ascertained from histological sections

Parameter	Plane/location	*Hemicordulia tau*	*Aeshna mixta*
Lens aperture (μm)	Horizontal	480	630
	Vertical	370	430
Lens external radius of curvature (μm)	Horizontal	300	455
	Vertical	250	330
Lens axial thickness (μm)	—	475	510
Clear zone depth (μm)	—	14 (7–20)	14 (10–20)
Rhabdom length (μm)	Centre	230	200
	Periphery	70	70
Rhabdom diameter (μm)	Distal	5 (5–8)	6.5 (6–7)
	Proximal	11 (10–12)	17 (15–19)
Rhabdom separation (μm)	Distal	7 (6–9)	8.5 (8–10)
	Proximal	15.5 (14–20)	19.5 (14–27)

Where possible a mean value is given, with ranges indicated in brackets. Separate entries in plane or location are given where values differ substantially across the eye. In the case of rhabdom length, values are given across the vertical plane: rhabdom length remains approximately constant across the horizontal plane. Rhabdom diameter was approximated by determining the diameter of a circle required to surround the entire rhabdom. Rhabdom separation indicates distance from centre of rhabdom complex to closest neighbouring rhabdom.

3.2.2. Retinal structure and relationship to lens

The inner lens surface is bounded by darkly pigmented corneagenous cells which act as a mobile iris during light adaptation (Stavenga, Bernard, Chappell, & Wilson, 1979). Retinula cells lie directly behind the corneagenous cells; there is essentially no clear zone in dragonfly ocelli. Three retinula cells contribute to a single rhabdom, which are shaped as tri-radiate stars (Stange et al., 2002). Rhabdom diameter is smallest at the rhabdom tip, and increases by a factor of two or more toward the base of the rhabdom (Table 1). Adjacent rhabdoms are generally well separated from each other, though often in an irregular manner.

As with the shape of the lens, the shape of the retina is also distinctly bilobed (Fig. 2A). Rhabdoms are, however, continuous over the midline of the lens with the exception of the ventral most surface of the retina. From comparison of vertical and horizontal sections through the eye (Fig. 3), it is apparent that the length of the rhabdoms changes throughout the retina. In the horizontal plane, rhabdom length remains approximately uniform over the width of the retina. In the vertical plane, however, rhabdoms are approximately three times longer at the centre of the eye than at the ventral and dorsal extremes (Table 1).

Near the base of the rhabdom, retinula cells are cupped by reflecting tapetal cells, which appear brown in thick sections (Fig. 3C). Proximal to the reflecting pigment layer lies a densely packed layer containing the retinula cell axons and nuclei. Axons project through a thick membranous sheath which defines the retinal boundary. Thereafter they enter a synaptic plexus area, where synapses with second-order neurons are formed.

3.3. Imaging by the excised lens

3.3.1. Focal length and astigmatism

Utilising the hanging-drop method to directly examine the image produced by the median ocellar lens immediately reveals a peculiar feature, namely that the image produced by the lens is not a single image, but rather is split laterally into left and right halves (Fig. 4). Rays entering the median ocellus from within 10° to 15° of visual space in front of the eye are split, such that rays entering the lens across a vertical transect produce a single image, while rays entering the lens across a horizontal transect form one or more images (Fig. 4A). This phenomenon is only apparent for rays entering the eye at an angle close to parallel with the optical axis of the lens; objects positioned off-axis produce only a single image. This is demonstrated in Fig. 5B where a wide field radial pattern was imaged through the lens: bilateral splitting is only observable near the central region of the image.

In the only available account of imaging through the dragonfly ocelli, Stange et al. (2002) describe the image

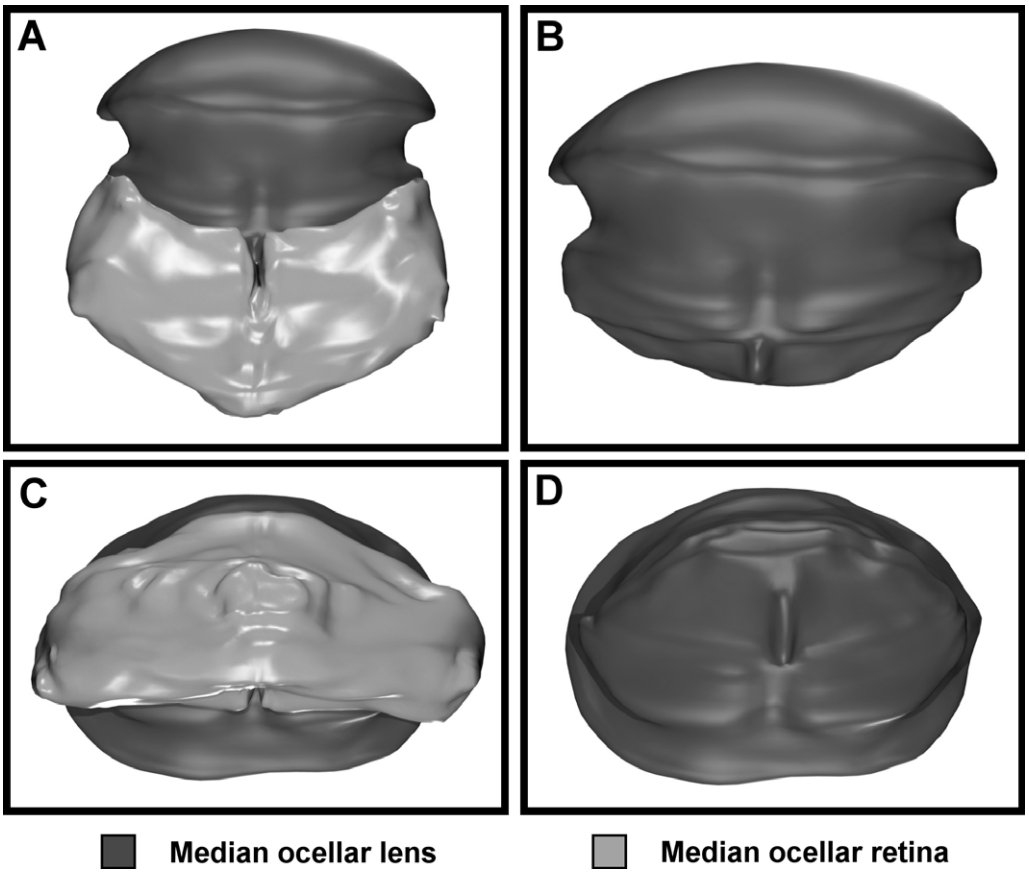

Fig. 2. Three-dimensional reconstructions generated from serial sections through the median ocellus of *Hemicordulia tau*. (A and B) Ventral view of the median ocellus with and without retina, respectively. (C and D) Posterior view of the median ocellus with and without retina, respectively. Note in particular the elliptical shape of the lens and the bilobed structure of the ventral inner lens surface. Dorsally, the inner lens surface becomes more continuous, with a pronounced protrusion extending posteriorly from the inner lens surface.

produced by the median ocellus of *Hemicordulia* as strongly astigmatic. The image of a point source of light appeared as a well focused horizontal streak at the vertical focal plane, and a poorly defined circle at the horizontal focal plane. The exact locations of foci could not be defined. However, the vertical focal plane was described as lying close to the inner surface of the lens, with the horizontal focal plane lying 200 μm behind the vertical focal plane. This finding would appear to sit well with the anisotropy in the external curvature of the lens in the horizontal and vertical planes.

Clearly, the results described here differ substantially from those described by the earlier study. If the lenses examined here were strongly astigmatic, the images shown in Fig. 4 would not be possible, as both the horizontally and vertically modulated features of the stimulus would not be in focus at the same location. Given the elliptical shape of the lens it is somewhat surprising that the results described here, in fact, support the opposite conclusion; namely that the lens is quite stigmatic.

From examination of the optical properties of the median ocellar lenses of both *Hemicordulia* and *Aeshna*, a number of salient parameters of the eye were established and these are given in Table 2. The back focal distance (BFD) of the lens is defined as the distance between the inner surface of the lens and its focal plane in water. Calculating this distance for horizontally and vertically modulated gratings yields a quantitative analysis of the amount of astigmatism present in the eye. In *Hemicordulia*, mean BFDs of 129 and 142 μm were obtained for vertically and horizontally modulated stimuli, respectively, the difference between which was not found to be significant (one-tailed *t*-test, $P < 0.05$), indicating that the eye is stigmatic. Back focal distances are slightly longer in *Aeshna*, which may be a reflection of the generally larger eye size in this species. In this case BFDs of 169 and 174 μm were obtained for the vertical and horizontal planes, respectively. Again these values did not significantly differ (one-tailed *t*-test, $P < 0.05$). In both *Hemicordulia* and *Aeshna*, the lens forms a focal plane within the retinal layer, close to the base of the rhabdoms (Fig. 5).

Given the above observations, the proximal focal streak observed in the dragonfly median ocellus (Stange et al., 2002, Fig. 5A) is unlikely to be the primary image of an astigmatic system, but resulted from observing the multiple images of a point source close to the optical axis of the lens. Indeed the streak has an irregular appearance, and the image of a point source appeared increasingly circular

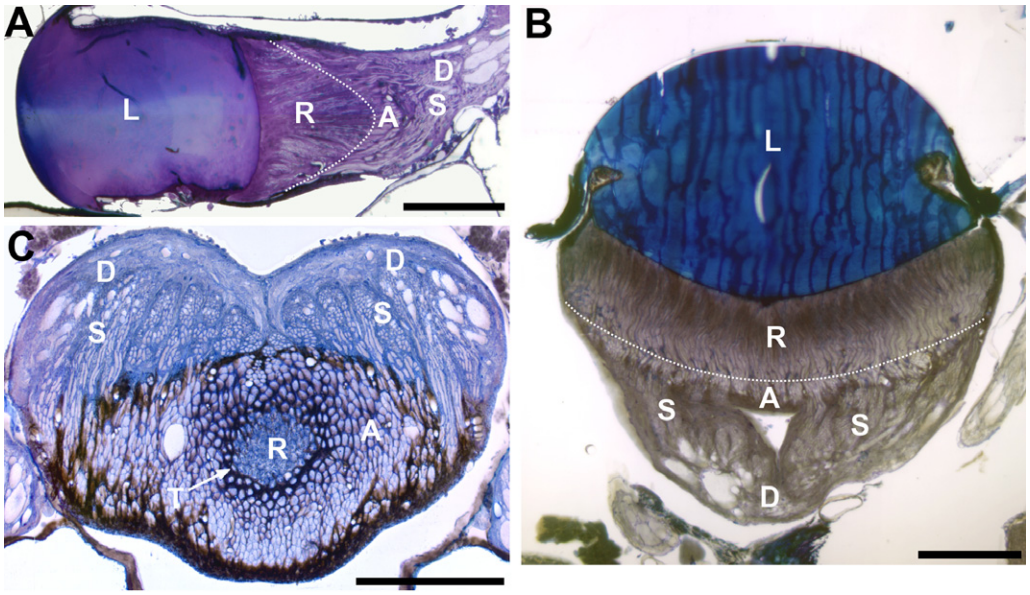

Fig. 3. Light micrographs of the dragonfly median ocellus. Section in (A) is a semi-thin section taken in a vertical orientation through the midline of the lens of *Hemicordulia tau*. Note in particular the strongly curved external surface of the lens (*L*) and the rapid decrease in rhabdom length towards the ventral and dorsal extremes of the retina (*R*) (dashed white line marks proximal limit of rhabdoms). Section in (B) is a thick (15 μm) section taken in an approximately horizontal orientation through the median ocellus of *Aeshna mixta*. In the horizontal plane rhabdom length remains constant over the width of the eye (dashed line). (C) A thick (15 μm) frontal section through the base of the retina of *Hemicordulia tau*. Rhabdoms are visible only near the centre of the retina, where they are surrounded by reflecting tapetal pigment (*T*) which appears brown in thick sections. Retinula cell axons (*A*) project through the retinal sheath (dark brown layer surrounding retina) to enter the synaptic plexus area (*S*) where they synapse with the dendrites (*D*) of second-order neurons. The synaptic plexus area does not form a well defined layer in the dorsal ocelli and is therefore difficult to define. Scale bars: all 200 μm. (For interpretation of the references of color in this figure legend, the reader is referred to the web version of this article.)

when moved from the optical axis of the lens toward the periphery (unpublished observation). Thus it appears that the elongated streak lying close to the inner surface of the lens corresponds to the actual focal plane, described here as lying 136 μm behind the inner lens surface. The origin of less well defined vertical streaks, observed by Stange et al. (2002, Fig. 5B) at a position of 200 μm behind the primary focal plane, is unclear.

3.3.2. Image quality and astigmatism

Although the locations of the respective focal planes do not differ between vertically and horizontally modulated gratings, the quality of the images formed differs substantially (Fig. 6). Images of vertically modulated gratings are of much higher contrast than images of horizontally modulated gratings of the same wavelength. In *Hemicordulia*, vertically modulated gratings yielded a significantly higher maximum spatial cut-off frequency of 1.19 cycles/degree, compared to 0.77 cycles/degree for horizontally modulated stimuli (one-tailed *t*-test, $P < 0.05$). In *Aeshna*, vertically modulated gratings similarly resulted in higher spatial cut-off frequencies (1.31 cycles/degree) than horizontally modulated gratings (0.78 cycles/degree). In this case, MTFs varied considerably between lenses, especially when analysing horizontally modulated stimuli, and this difference was not found to be significant (one-tailed *t*-test, $P < 0.05$).

Fig. 6B shows the spatial cut-off frequency as a function of distance behind the median ocellar lens of *Hemicordulia*. Vertically modulated gratings produced a strongly curved function, while horizontally modulated gratings produced a much flatter curve and lower maximum value: horizontally modulated features of the world are imaged poorly by this lens.

3.4. Ray tracing and theoretical description

3.4.1. Refraction by the inner lens surface

Two factors about the optical properties of the dragonfly median ocellus are somewhat puzzling. Firstly, how does the lens form a split image near the optical axis? Secondly, how does an elliptical lens with a larger aperture and radius of curvature in the horizontal direction than in the vertical direction, produce a stigmatic image? One possibility is that the bilobed nature of the inner lens surface accounts for both of these unusual properties. To test this hypothesis, rays were traced through two models of the median ocellus of *Hemicordulia* that described the lens in two-dimensional cross-section in either the vertical or the horizontal plane.

In the vertical plane, both the outer and inner surfaces of the lens were described by single semi-circles. In the horizontal plane, the outer surface of the lens was described by a single semi-circle, while the inner lens surface was described by two circle segments of equal radius, such that the inner lens surface attains a binary shape. The results of ray tracing through such a lens system are given in Fig. 7. From this, it can be seen that rays entering the lens in the vertical plane are refracted through the lens system to a sin-

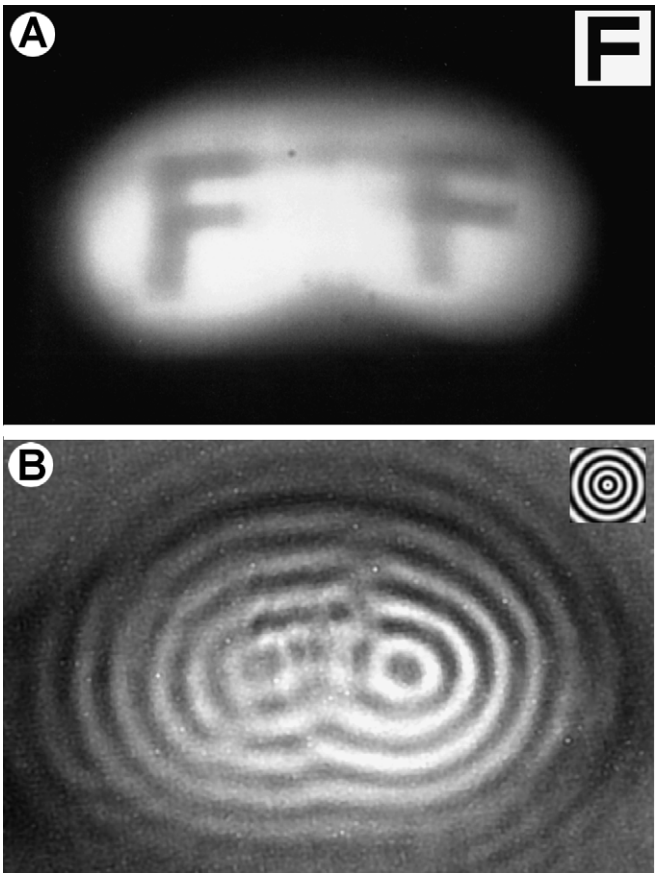

Fig. 4. The image splitting nature of the dragonfly median ocellus. Insets show representations of object patterns actually used. (A) The image of a single 'F' (inset) seen at the focal plane of the median ocellar lens of *Aeshna*. The image is split by the lens across the horizontal plane so that two images are observed. (B) shows an image of an angularly corrected radial pattern (inset) of 5° spatial wavelength as seen through the median ocellus of *Hemicordulia*. Bilateral splitting is observable, but only over the central region of the image.

gle point of focus (or more accurately point spread function) behind the inner lens surface. In the horizontal plane, however, the refractive index difference between the inner lens surfaces and the surrounding medium (taken as 1.5 and 1.34, respectively), together with the curvature of the inner lens surfaces, is sufficient to bilaterally split rays of low incidence angle into at least two points of focus. As the angle of the incoming rays increases, the majority of rays becomes incident upon only one of the two inner surfaces and a single dominant focal point emerges.

Quantitatively determining the angle at which incoming rays form a single, rather than multiple, points of focus is difficult as by nature this requires some subjective judgement. It is sufficient to say that multiple foci become markedly more indistinct as the angle of incidence increases from 5 to 15° from the optical axis of the eye. This corresponds well to the observation that multiple images are observed only for objects subtending a range of ±5°–7.5° from the optical axis. A horizontally extended object will therefore be imaged worst near the optical axis (where image splitting occurs), and best toward the periphery of the eye. This prediction also fits well with images observed through the excised median ocellar lens (Fig. 4).

The bilobed nature of the inner lens surface also results in a substantial shortening of the focal length of the lens in the horizontal plane. In *Hemicordulia*, for example, while the outer surface of the lens is more strongly curved in the vertical plane than in the horizontal plane (Table 1), each bilateral half of the inner surface of the lens has a much smaller radius of curvature (215 μm) in the horizontal plane, than the radius of the entire inner surface in the vertical plane (385 μm). Therefore, it can be predicted that the inner surface accounts for more of the refractive power of the lens in the horizontal plane than in the vertical plane, thereby cancelling out some of the astigmatism present in the outer lens surface. This may be tested by determining theoretical focal lengths from thick lens optics formulae (Eq. (4)). Using the values given in Table 1, with refractive indices n_1:1; n_2:1.5; and n_3:1.34, it can be shown that if refraction at the inner surface was negligible, then focal lengths of 575 and 785 μm would be expected in the horizontal and vertical planes, respectively. Accounting for refraction at the inner surface, however, gives much reduced values of 475 and 495 μm, respectively. Reduction of focal length is proportionally greater in the horizontal plane than in the vertical plane. In other words, the power ratio of the first to second interfaces is 1:0.21 when considering the lens in the vertical plane, which increases to 1:0.45 when considering the lens in the horizontal plane. It must be noted that using Eq. (4) to calculate the theoretical focal length of this lens is necessarily a simplification, given that the inner surface of the lens is of a geometrically complex shape. However, the focal lengths given by this equation are consistent with focal lengths obtained by ray tracing, and therefore this appears to be a reasonable simplification.

3.4.2. Evidence for gradients of refractive index

As described above, calculating the focal length of the median ocellar lens of *Hemicordulia* from Eq. (3) gives values of 475 and 495 μm in the vertical and horizontal planes, respectively. However, experimental measurement of the focal length by transverse magnification (Eq. (1)) yielded the much lower mean value of 299 μm. If the lens is homogeneous, this short focal length would require the lens to have a refractive index of approximately 1.79, which is exceedingly high for any known biological substance. Such a short focal length may be obtained if the refractive index of the lens is not homogeneous, but rather is graded such that the centre of the lens is of higher refractive index than the periphery (Land, 1981). If we consider the median ocellus as a simple sphere with a radius of curvature of 300 μm, then the focal length to radius ratio becomes 1. Fletcher, Murphy, and Young (1954) show that in air, a sphere with a correctly graded refractive index could achieve this ratio with a central refractive index of only 1.41, a value much more feasible by biological means.

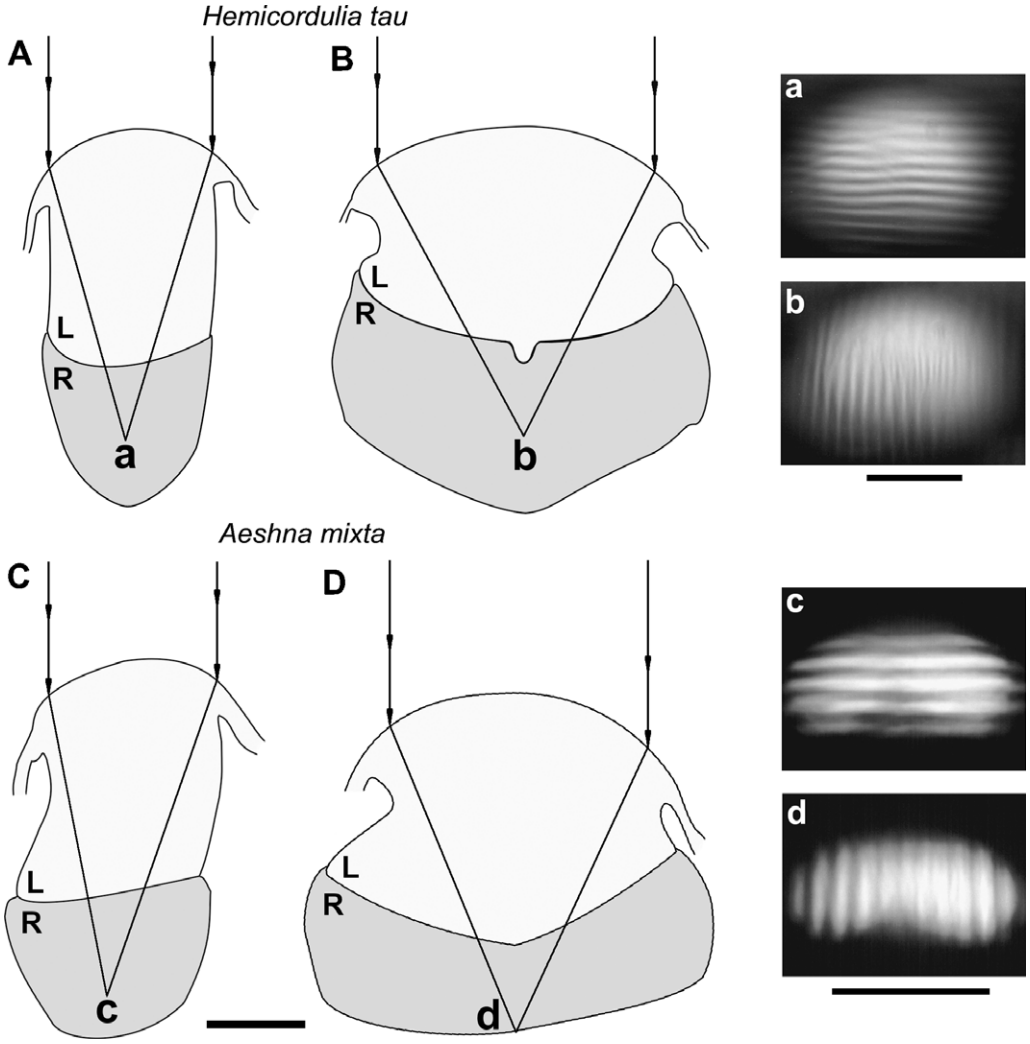

Fig. 5. Schematic representation of focal plane location in the dragonfly median ocellus. Outlines of lens (*L*) and retina (*R*) were traced from sections of *Hemicordulia* and *Aeshna*, in the vertical (A and C) and horizontal (B and D) planes. Focal planes lie at the location of convergence of two parallel rays. Gratings of 5° (a and b) or 4° (small field stimulus, c and d) spatial wavelength imaged through the lens at the focal plane are shown on the right. Note that vertically, modulated gratings are better resolved by the median ocellar lens than horizontally, modulated gratings, but that both focal planes are located in approximately the same location. Scale bars: all 200 μm.

Table 2
Optical properties of the dragonfly median ocellus

Parameter	Plane	*Hemicordulia tau* (6)	*Aeshna mixta* (5)
Focal length (μm)	Horizontal	300 ± 10	389 ± 32
	Vertical	298 ± 30	401 ± 66
BFD (μm)	Horizontal	142 ± 36	174 ± 40
	Vertical	129 ± 20	169 ± 29
V_c (cycles/degree)	Horizontal	0.77 ± 0.23*	0.78 ± 0.45
	Vertical	1.19 ± 0.36*	1.31 ± 0.51
F-Number	Horizontal	0.63	0.62
	Vertical	0.81	0.93
Optical sensitivity (μm^2 sr)		31.5	55.5

Values for spatial cut-off frequency (V_c) were obtained from the focal plane of the lens. Bracketed values give the number of animals used for analysis. *Asterisks* indicate a significant difference in values between the horizontal and vertical planes ($P < 0.05$).

A direct test for the presence of refractive index gradients within a lens can be performed by the use of interference microscopy. To this end, frontal sections of the median ocellus of *S. danae* were examined under an interference microscope with the results shown in Fig. 8. These images show clear evidence for the existence of gradients of refractive index within the lens. The form of the gradient, however, is rather complex. Sections taken towards the anterior of the lens reveal a relatively smooth gradient, with refractive index increasing from the periphery of the lens to the centre. Progressing posteriorly, a central core of high refractive index becomes prominent. The core is surrounded by a peripheral ring of lower and only slightly graded refractive index. Unfortunately, due to uncertainty in the thickness of the sections, it was not possible to determine the refractive indices of the lens with accuracy.

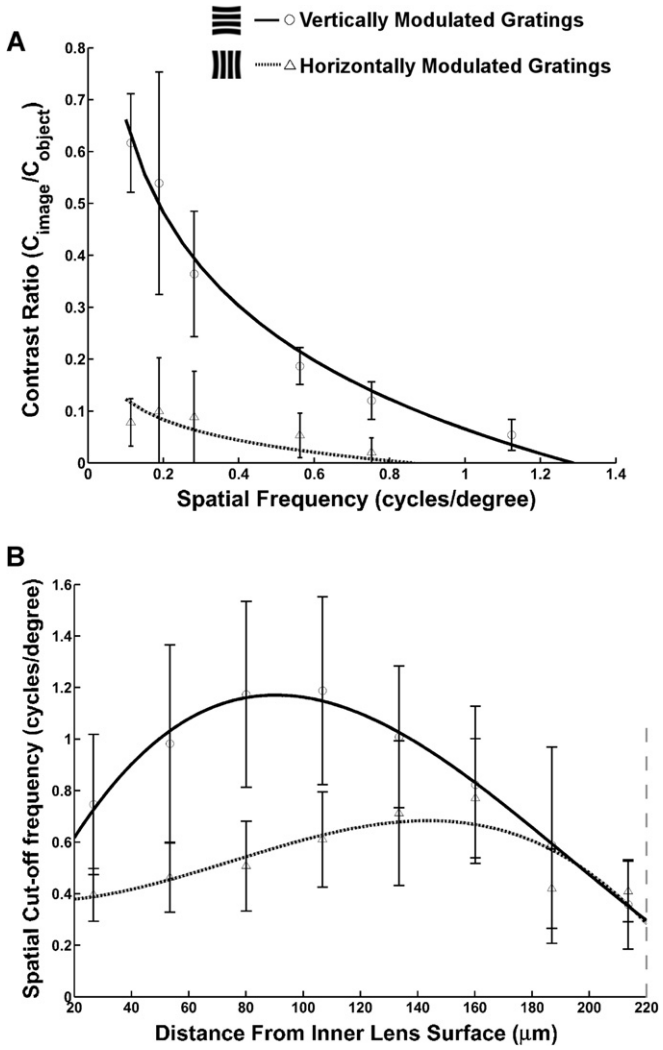

Fig. 6. Modulation transfer functions and spatial cut-off frequency functions for the dragonfly median ocellus. (A) MTFs for horizontally and vertically modulated gratings at the focal plane of the median ocellar lens of *Aeshna*. Contrast for vertically modulated gratings is much higher than for horizontally modulated gratings. (B) gives the spatial cut-off frequency of *Hemicordulia* at various points of defocus behind the inner lens surface. Although image contrast, and hence spatial cut-off frequencies, are higher for vertically modulated gratings, both orientations result in curves which peak at nearly the same location, indicating little astigmatism. Legend indicates the orientation of the stimulus used to generate MTFs or spatial cut-off frequency functions. *Dashed grey line* in (B) indicates the proximal limit of the rhabdom layer.

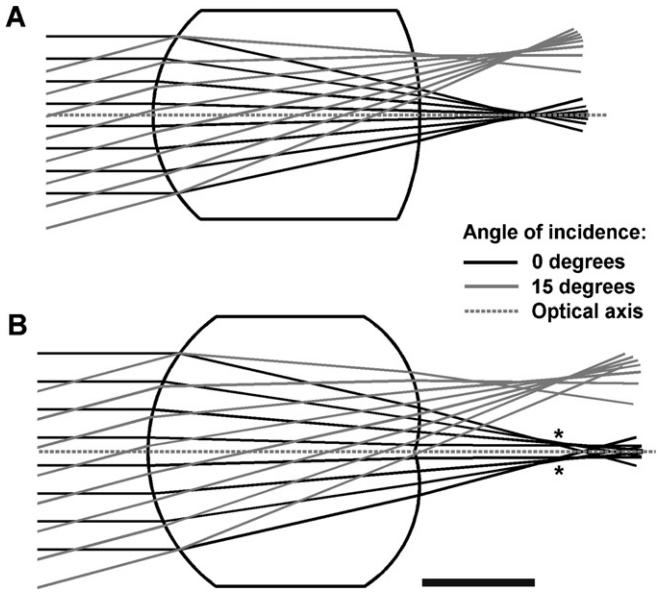

Fig. 7. Bilateral imaging by models of the dragonfly median ocellar lens. Incoming rays with an incidence angle of either 0° or 15° are traced through the lens. (A) The lens as modelled from cross-sections in the vertical plane. As the inner lens surface is continuous, incoming rays always form a single focal point. (B) The lens in the horizontal plane. When incoming rays are close to parallel with the optical axis, each lateral half of the median ocellus refracts rays such that two points of focus (*) are formed. At larger angles of incidence no clear distinction of focal points is observed; the majority of incoming rays tends to form a single blur circle. Scale bar: 200 μm.

Estimating section thickness as 14 μm gives refractive index values of 1.47 at the centre and 1.40 at the periphery.

3.4.3. Angular sensitivity functions

The models of the median ocellar lens of *Hemicordulia* described above were extended to simulate a layer of retinula cells behind the lens surface. The retinal layer consists of a number of rhabdom units, which are modelled as cross-sections of tapered cylinders thus appearing pyramidal in shape. Parameters describing the rhabdom arrays were based on values determined from histological sections as given in Table 1. Additionally, a set proportion of the rhabdom length could be ensheathed by reflecting tapetum, which directly surrounds the base of the rhabdom. From light microscopy of thick resin embedded sections it was estimated that 27% of the rhabdom length was sheathed by tapetum; unless otherwise stated, this is the value that is used. Scale diagrams of the model in the vertical and horizontal planes are shown in Fig. 9A and D.

By tracing rays through the model at various angles of incidence to the lens, angular sensitivity functions of every rhabdom in the array could be generated. Due to the larger diameter of the eye in the horizontal plane, the rhabdom array in this orientation is larger. Additionally, the shorter *F*-number and larger retinal area of the eye in the horizontal plane results in a larger field of view. Hence, the range of angles over which rays are traced is greater in this plane.

Fig. 9B and E show the outputs of the ray tracing model for rhabdoms in the vertical and horizontal planes respectively. In the vertical plane, angular sensitivity functions are sharply peaked and generally remain of similar shape throughout the eye. The tapetally sheathed bases of rhabdoms are located progressively closer to the inner lens surface with increasing distance from the central axis. Consequently, rhabdoms become increasingly underfocused, and angular sensitivity functions become wider and flatter towards the periphery of the eye. Acceptance angles of rhabdoms close to the central axis are approximately 3.6°, compared to 6.8° for rhabdoms at the dorsal

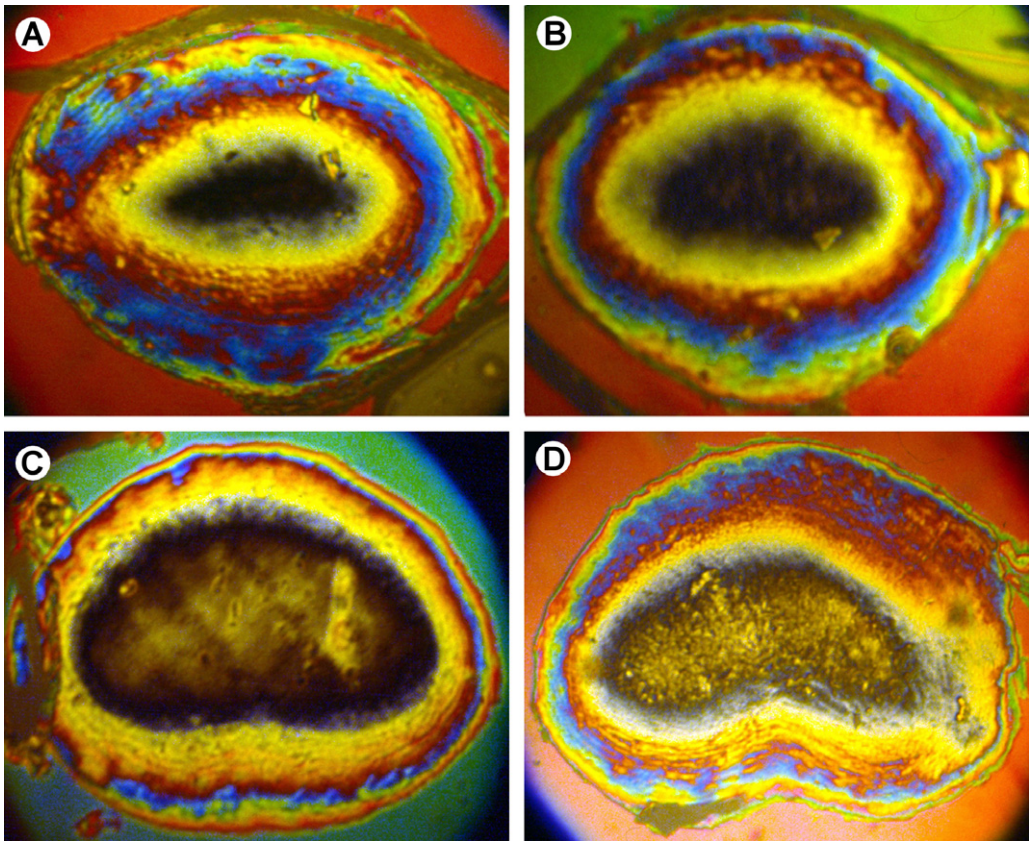

Fig. 8. Frontal sections of the median ocellar lens of *Sympetrum danae* under interference microscopy. Sections progress from the anterior of the lens (A) to the posterior of the lens (D). Variation in colour corresponds to changes in refractive index, with darker colours indicating a higher refractive index. In sections taken towards the anterior of the lens, a smooth gradient of refractive index is observed, with increasing refractive index towards the centre of the lens. In sections taken further posteriorly, the lens appears to consist of two elements; a central core of high refractive index and an outer ring of lower refractive index. Refractive index is estimated to be graded from 1.40 at the periphery, to 1.47 within the central core.

and ventral extremes. By summing the amount of light absorbed by each rhabdom in the array to light rays from all angles of incidence (i.e. an extended light source), the total light absorption of each rhabdom can be calculated. In the vertical plane, total absorption falls off towards the periphery of the eye in correlation with decreasing rhabdom length (Fig. 9C).

The situation is essentially reversed in the horizontal plane. In this case, rhabdom length remains constant over the width of the eye. However, because of the image splitting properties of the lens, rhabdoms near the centre of the eye have low maximum sensitivity values, as light focused close to the optical axis of the eye is blurred over a wide area of the retina (Fig. 9E). In correlation with the image splitting nature of the lens, rhabdoms near the centre of the eye show double peaked angular sensitivity functions and large acceptance angles of up to 14.1°. As the angle of incident light increases, the lens forms a single region of focus and concomitantly acceptance angles decrease. Rhabdoms near the periphery can have acceptance angles of as low as 6.4°. Note that while maximum sensitivity values are lower for rhabdoms near the centre of the array (Fig. 9E), the larger acceptance angles of these rhabdoms results in an equivalent light capturing capacity to more peripheral rhabdoms under illumination by an extended light source (Fig. 9F).

3.4.4. Optimality of tapetal sheathing

By varying the extent to which rhabdoms are sheathed by reflecting tapetum in the model, it is possible to observe its effect on light capture both across the entire retina and in individual rhabdoms, as well as its effect on the acceptance angles of individual rhabdoms. The results of such an experiment are shown in Fig. 10. For simplicity, this experiment only modelled changes in tapetal sheathing of rhabdoms in the vertical plane. Rays were traced from elevations of −15° to +15° and therefore only covered the visual field of the central-most rhabdoms in the array.

As can be seen from Fig. 10, increasing the extent to which rhabdoms are sheathed by reflecting pigment results in a decrease in both the amount of light absorbed by the entire retina, and by individual rhabdoms. The effect on light absorption is generally minor, with light absorption by the entire retina decreasing from a maximum value of 80% at zero tapetal sheathing (basal tapetum only), to 51 at 100% tapetal sheathing. The percentage of light absorbed by the central most rhabdom in the array decreases from 4.9% at zero tapetal sheathing, to 2.9% at

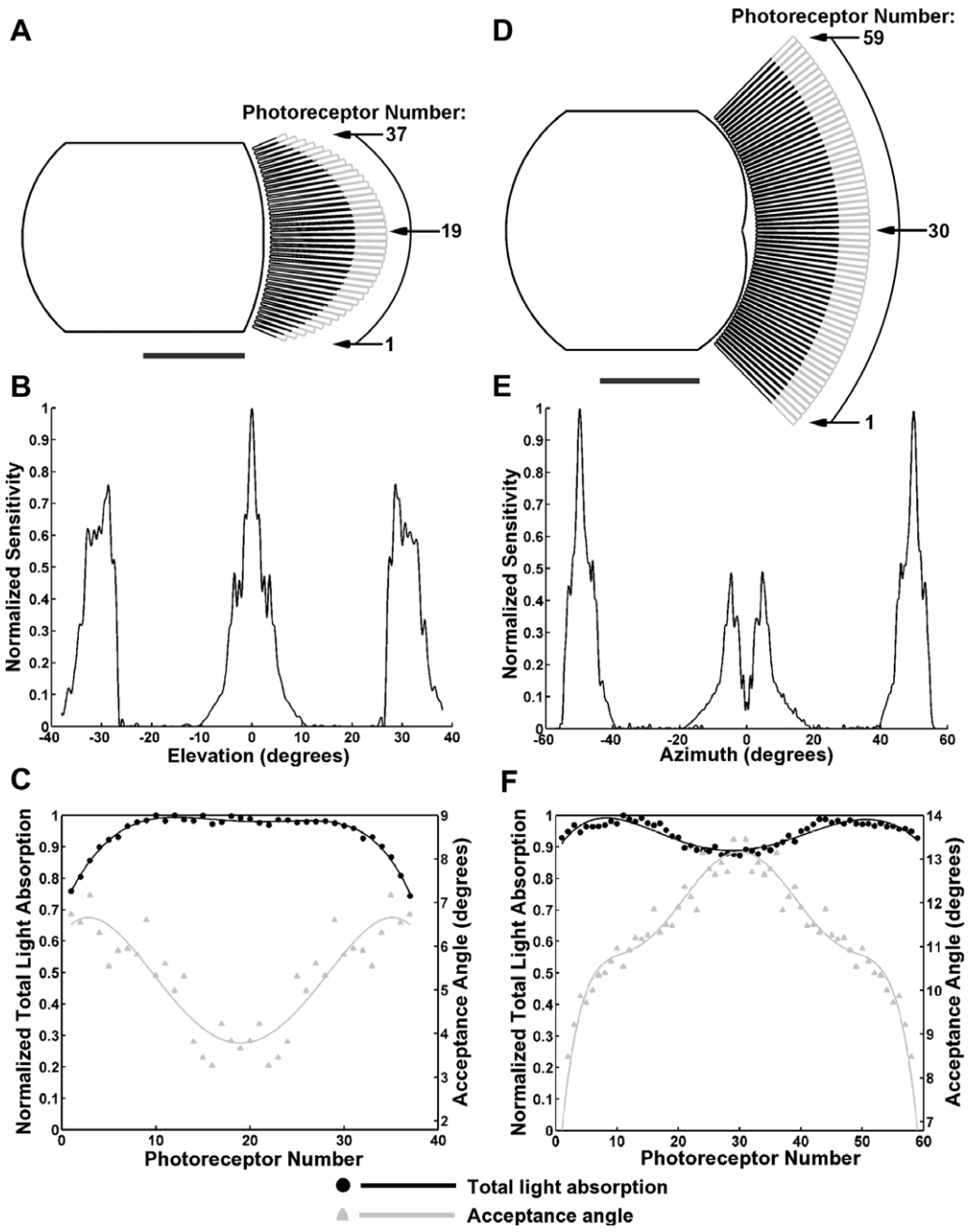

Fig. 9. Ray tracing through the median ocellus of *Hemicordulia tau*. In the vertical plane (A) the rhabdom array (*black and grey trapezoids*) consists of 37 rhabdoms with lengths that are modulated in a parabolic manner. Angular sensitivity functions were obtained by tracing over 18, 000 rays through the model, from −38° to +38° in elevation, and are shown in (B) for the three photoreceptors marked in (A). Rhabdoms positioned near the centre of the eye have smaller acceptance angles and higher peak sensitivity values than those near the periphery. (C) gives the acceptance angle and total light capture (normalised to highest value in the array) for all photoreceptors. Total light capture falls off towards the periphery of the array due to decreased rhabdom length. In the horizontal plane (D) the rhabdom array consists of 59 rhabdoms, the length of which remains constant. Angular sensitivity functions were obtained by tracing approximately 28,000 rays through the model, from −60° to +60° in azimuth, and are shown in (E) for the three photoreceptors marked in (D). Rhabdoms near the centre of the eye have lower peak sensitivities and double peaked receptive fields due to bilateral ray splitting by the optics. Peripheral rhabdoms have higher peak sensitivity and more restricted receptive fields. (F) gives the acceptance angle and total light capture (normalised to highest value in the array) for all photoreceptors. Light capture remains relatively constant throughout the array, with only a small decrease at the centre of the eye due to bilateral image splitting by the lens. In both models the proximal endings of the rhabdoms are sheathed by reflecting pigment (*grey lines* in (A and D)). Scale bars: 200 μm.

100% tapetal sheathing. The effect on resolution, however, is much more drastic. Acceptance angles are smallest, and hence resolution highest, at 30% tapetal sheathing (acceptance angle of 4.3°). Altering the extent of tapetal sheathing results in nearly a 5-fold difference in the range of acceptance angles observed, with acceptance angles at 100% tapetal sheathing reaching a value of 20.9°. A value of 27% sheathing (the mean value found in the ocelli of

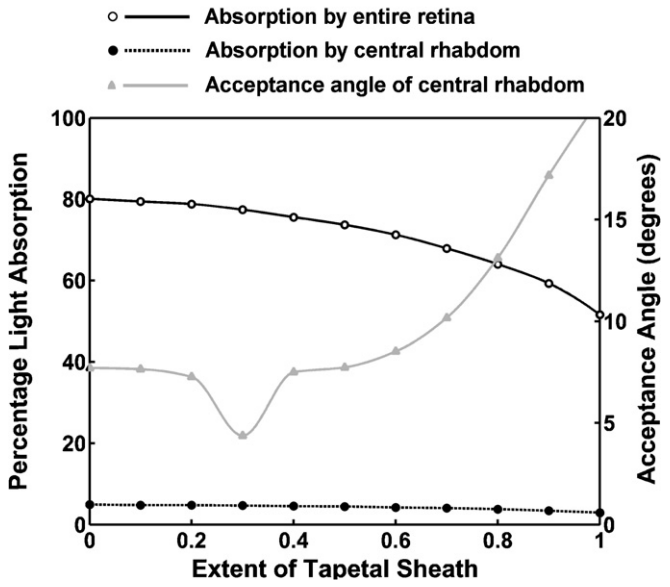

Fig. 10. Resolution and sensitivity as a function of the extent of tapetal sheathing. Rays were traced through the median ocellus in the vertical plane only. As the extent of tapetal sheathing increases, light absorption by the entire retina, and by the central rhabdom in the array decrease. Resolution is best (lowest acceptance angle) when the extent of tapetal sheathing is 30%. A greater or lesser extent of tapetal sheathing significantly degrades resolution.

Hemicordulia) has a minor detrimental effect on the sensitivity of the eye when compared with 0% tapetal sheathing, but dramatically improves resolution. These results suggest that the degree of tapetal sheathing found in dragonfly ocelli is an adaptation to maximise the available resolution.

3.4.5. Estimates of sensitivity

The Land sensitivity equation Eq. (5) combines the most salient features of an eye, namely its aperture, focal length and rhabdom dimensions, to given an estimation its light capturing ability. Using Eq. (5) to calculate the optical sensitivities (S) of the dragonfly median ocellus, from the mean values given in Tables 1 and 2 at the centre of the ocellar retina (longest rhabdom lengths), with an absorption coefficient of 0.0067 μm^{-1}, yields the remarkably high values of 31.5 μm^2 sr for the median ocellus of *Hemicordulia* and 51.5 μm^2 sr for the median ocellus of *Aeshna*. For comparison, dragonfly compound eye ommatidia, despite possessing large diameter facets and exceptionally long rhabdoms (exceeding 1 mm in dorsal regions of the eye (Labhart & Nilsson, 1995; Laughlin & McGinness, 1978)), achieve optical sensitivity values of only 0.29–1.7 μm^2 sr (from values given in Labhart & Nilsson (1995)).

4. Discussion

4.1. Properties of the lens

We find here that the dragonfly median ocellar lens forms a relatively stigmatic image close to, or within, the rhodopsin containing area of the retina. The elliptical shape of the lens and retina, in combination with stigmatic imaging, results in a wider field of view and higher sensitivity in the horizontal plane than in the vertical plane.

Resolution, however, is better in the vertical plane than in the horizontal plane, as was originally, proposed by Stange et al. (2002). With spatial cut-off frequencies of 0.77–1.31 cycles/degree, the median ocellar lens is capable of resolving objects down to spatial wavelengths of 1.3° and 0.7° in the horizontal and vertical planes, respectively.

The image formed by the median ocellar lens contains two somewhat unusual properties. First the image produced is stigmatic, despite a smaller radius of curvature of the outer lens surface in the vertical plane than in the horizontal plane. Second the image formed is bilaterally split across the midline of the eye in the horizontal plane. Both unusual imaging properties may be accounted for by the bilobed structure of the inner surface of the lens. These effects could be accurately reproduced by ray tracing through a model lens of similar geometry as the median ocellar lens of *Hemicordulia*.

Note, however, that refraction by the inner lens surface may not fully account for image splitting or stigmatic optics in the median ocellus, as the inner lens surface is not bilobed over its entire extent. The dorsal half of the lens is decidedly flatter than the ventral half, and in this region the bilobed structures are replaced by a cuticular protrusion which extends outwards from the lens surface (see Fig. 2). The effect of this protrusion on the image formed by the lens is difficult to predict, but judging by its shape, it is not likely to contribute to bilateral splitting or stigmatic imaging.

An alternative explanation for both phenomena is that these properties arise from the form of refractive index gradients within the lens. Evidence for refractive index gradients is given both directly by interference microscopy, and indirectly by comparison of theoretical and determined focal lengths. The lens consists of a homogeneous core, which increases in size towards the posterior of the lens, and an outer peripheral ring which surrounds the core and contains a refractive index gradient. Fig. 8 suggests that the homogeneous core of the lens forms a bilobed shape toward the posterior region of the lens. It could well be imagined that such a shape will contribute to the complex optical properties of the lens.

Lenses with graded refractive indices are relatively common in the eyes of fish (e.g. Jagger & Sands, 1996; Kröger, Campbell, Munger, & Fernald, 1994), where the power of the corneal interface is much reduced due to immersion in water, and because they have the advantage of simultaneously decreasing the focal length of the lens and allowing for complete correction of spherical aberration. In the simple eyes of terrestrial invertebrates, however, such graded refractive index lenses are rare. Refractive index gradients have been postulated in the posterior eye of the semi-aquatic spider *Dolomedes aquaticus* (Williams, 1979), and in the stemmata of *Perga* (sawfly) larva (Meyer-Rochow, 1974).

Notably, Blest and Land (1977) show the posterior median eye of the spider *Dinopis subrufus* to consist of two components; a soft peripheral ring of low refractive index, and an inner core of higher and graded refractive index.

Until recently, however, gradients of refractive index were generally considered to be confined to lenses where a relatively high degree of spatial resolution is required. Nilsson, Gislen, Coates, and Garm (2005) show that this cannot be the case in the lens eyes of the box jellyfish *Tripedalia cystophora*. Each of the four sensory clubs (rhopalia) of *Tripedalia* contains two lens eyes, both of which contain gradients of refractive index that either partially, or almost perfectly, correct for spherical aberration. Perplexingly, however, the retina in both eyes appears to be 'misplaced', such that it is located far closer to the inner lens surface than the focal plane. The retina thus receives a highly underfocused image, therefore resembling the underfocused ocelli of many insects (rev. Goodman, 1981). By ray tracing through the lens, Nilsson et al. (2005) were able to show that a combination of graded index optics and obliquely aligned rhabdoms produces receptive fields of very complex shapes. They proposed that in this case, the graded refractive indices in the lenses are an adaptation to achieve these complex receptive field shapes by simple optical means, whereas they are achieved in vertebrate visual systems only at a much higher level of processing. In the case of the dragonfly ocelli, we must also conclude that the morphologies of the lens and retina are adaptations to reduce the amount of neuronal processing required for their role.

4.2. Performance and limitations of the ray tracing model

A physiological representation of resolution in individual photoreceptors was obtained by tracing rays through a model of the dragonfly median ocellar lens and retina. The highest acuity rhabdoms were found to lie at the centre of the eye in the vertical plane, but the periphery of the eye in the horizontal plane. Taking the mean values from the model, acceptance angles in elevation (5.2°) are two times smaller than those in azimuth (10.3°). In general these results are quite consistent with the known properties of the median ocellus of *Hemicordulia* as determined by ophthalmoscopy (Stange et al., 2002) as well as intracellular electrophysiology of individual photoreceptors (van Kleef et al., 2005). However, the acceptance angles obtained by ray tracing are a factor of 2 or more smaller than the mean acceptance angles of 15° in elevation and 28° in azimuth given by van Kleef et al. (2005). There may be several reasons for this discrepancy, as discussed below.

First, the lens used in the model consisted of a homogenous refractive index, as the available data on refractive index gradients in the dragonfly median ocellar lens was not sufficient to permit accurate modelling. This results in the modelled lens having a substantially longer back focal distance (approximately, 210 μm) than the real lens of *Hemicordulia* (136 μm). A shorter back focal distance may result in higher acceptance angles due to the increased effect of optical cross-talk, and the less optimal nature of focal plane location with respect to tapetal sheathing.

Second, the diameter of the tapetal sheath in the model is underestimated. Rhabdoms in the dragonfly ocelli are tri-radiate star shaped and are formed by the fusion of three photoreceptors. Tapetal sheathing does not wrap around the rhabdom itself, as modelled here, but rather wraps around all three photoreceptors contributing to the rhabdom (Stange et al., 2002). The diameter of the tapetal sheath may therefore be larger than the diameter of the rhabdom. A larger diameter tapetal sheath will trap light from a larger solid angle, thereby increasing acceptance angles.

Third, and probably most importantly, there is good reason to believe that there is neural coupling between photoreceptors themselves, as well as between photoreceptors and second-order neurons in the ocellar plexus (Chappell & Dowling, 1972; Dowling & Chappell, 1972; Klingman & Chappell, 1978; Simmons, 1982; Stone & Chappell, 1981). Neural coupling can greatly improve the sensitivity of the eye and the signal-to-noise ratio of photon transduction, but at the cost of resolution.

Lastly, although van Kleef et al. (2005) give mean acceptance angles of 15°–28°, values as low as 4°–9° in elevation and azimuth, respectively, were recorded. These values closely match the smallest acceptance angles determined from the model and suggest that photoreceptors are capable of quite restricted receptive fields, possibly when, for example, resolution is not compromised by neural coupling. It is also possible that the mean values provided by van Kleef et al. (2005) underestimate photoreceptor resolution, as recordings from electrode damaged photoreceptors may have artificially skewed the mean value.

4.3. Adaptations for resolution

While it is apparent that the 'inappropriate' placement of the retina precludes the possibility of high resolution form vision by the dragonfly median ocellus, the location of the focal plane close to the point at which tapetal sheathing begins suggests that some level of resolution is desirable. Even relatively small changes in the extent of tapetal sheathing have a large effect on the acceptance angle of rhabdoms, but only a minor effect on light capture (Fig. 10). A similar conclusion was drawn by Warrant and McIntyre (1991), who analysed the effect of the extent of pigment sheathing on resolution and light capture in models of the superposition eyes of several species of dung beetle. They found that when the eye is poorly focused, partial sheathing with reflecting pigment results in optimal resolution and light capture.

The detrimental effect of optical cross-talk is also minimised by the tapered shape of the rhabdoms, which have the smallest volume at the distal tips and expand proximally. Locating the bulk of the photopigment near the base

of the rhabdoms reduces the fraction of light absorbed from rays passing through 'non-target' rhabdoms.

4.4. Factors affecting resolution

A factor not accounted for here is that dragonfly ocelli, as is the case with all other dorsal ocelli, show massive convergence from first- to second-order neurons. In the median ocellus, 1500 photoreceptors converge onto a total of eleven large second-order neurons (L-neurons), and 30 or so small second-order neurons (S-neurons) (Berry et al., 2006; Chappell, Goodman, & Kirkham, 1978; Patterson & Chappell, 1980). Such an anatomical arrangement precludes the possibility of high resolution retinotopic mapping of the world to higher order visual centres. This would not, however, prevent the possibility of local processing of spatial information within the ocellar neuropile. From our recent work on the second-order neurons of the dragonfly median ocellus, it is apparent that spatial imaging is preserved after convergence from photoreceptors to ocellar interneurons (Berry et al., 2006). Indeed, acceptance angles of median ocellar L-neurons may be as small as 15° in elevation, which approaches the limit set by the acceptance angles of individual photoreceptors (van Kleef et al., 2005).

4.5. Adaptations for sensitivity

As the dragonfly median ocellar retina is located directly behind the inner lens surface, achieving focused optics in this system requires a very short focal length. A short focal length relative to the aperture of the lens (low *F*-number $\left(\frac{f}{A}\right)$, where f is the focal length of the lens and A its aperture) confers several advantages on an optical system, including; allowing a large depth of focus, allowing a large field of view, and allowing very high sensitivity.

In addition to *F*-numbers as low as 0.62, sensitivity in the dragonfly median ocellus is further enhanced by long, and relatively large diameter photoreceptors. These two factors contribute to the remarkably high optical sensitivity values of 31.5 and 51.5 μm^2 sr obtained for *Hemicordulia* and *Aeshna* respectively. These values are some 19–178 times larger than comparable values obtained from dragonfly compound eye ommatidia. Dragonfly ocelli are also 5–11 times more sensitive than locust ocelli (see accompanying publication), suggesting that high sensitivity is especially important in the former.

High sensitivity confers a number of advantages on an eye, the most obvious of which is probably functioning in low light conditions. Some behavioural evidence of this capacity has been provided by Stange (1981), who describes ocellar mediated dorsal light responses in *Hemicordulia* as being fully functional even at luminance levels below those of moonless nights. What is puzzling, however, is that an eye of this sensitivity is found in a predominantly *diurnal* animal. While the nocturnal behaviour of dragonflies is not well understood and it is entirely possible that dragonflies are active at night (from our own observations, and those of Mobbs, Guy, Goodman, & Chappell (1981), it is clear that at least some species of Aeshnidae are on the wing at dusk), it appears that many species of dragonflies are only active in bright light conditions. On a bright sunny day, the drop in illumination level caused by a cloud drifting in front of the sun is sometimes all that is required for *Hemicordulia*, and several other species of dragonfly, to abandon foraging or territorial protection and settle down to roost in nearby foliage. Explanations proposing that the high sensitivity of the median ocellus is an adaptation for vision in dim light conditions therefore appear unlikely.

There are two other possibilities as to why a diurnal insect may require such a sensitive eye; namely contrast resolution and temporal resolution. Contrast resolution is essentially a measure of the number of intensity levels that can be distinguished by a photoreceptor mosaic. High contrast resolution requires high sensitivity because of the random nature of photon emission and absorption; the signal-to-noise ratio of a photoreceptor increases with increasing light intensity (Snyder, 1977; Snyder, Laughlin, & Stavenga, 1977). It is generally beneficial for an eye to capture as many photons as possible, as this allows discrimination between small contrast differences at relatively bright light levels, or larger contrast differences at dimmer light levels (Land, 1981). Temporal resolution is simply a measure of the "shutter speed" or "frame rate" of the receptor array, which is determined by the integration time of a photoreceptor. Photoreceptor integration times are typically short in flying insects, where rapid response times are critical and image blur while moving is problematic. Higher sensitivity therefore not only allows the discrimination of smaller differences in contrast, but also the ability to distinguish the same differences in contrast at shorter time intervals.

4.6. Functional consequences of eye design

Given that the resolution of the dragonfly median ocellus is relatively modest when compared with its very high sensitivity, it is reasonable to infer that this ocellus, as with locust ocelli, is geared towards sensitivity over spatial resolution. It is interesting to note that, in principle, a much higher spatial resolution could be obtained in the median ocellus without a loss in optical sensitivity by simply separating the retina from the lens with a clear zone. As this simple feature has not been included in the eye, we must conclude that the dragonfly ocelli do not require this degree of resolution for normal operation. In fact, such a solution may be disastrous for two reasons. First because, as Wilson (1978) notes, high light intensities focused onto the retina may lead to retinal damage, a very real problem in an eye of these dimensions. Locating the photoreceptors directly behind the lens surface may act as a diffusing mechanism which prevents high local concentrations of light (e.g. from the sun) from causing retinal damage. Second Snyder (1977) shows that the effect of angular motion on an eye is equivalent to a reduction in intensity by an

amount that is inversely proportional to the acceptance angle of its photoreceptors. Dragonflies are exceptionally, fast fliers, and are capable of body rotations around the yaw axis in the order of 2000°/s (N. Carey, personal communication). Relatively large receptive fields, combined with high temporal resolution, will allow the ocelli to maintain reliable signalling even during demanding manoeuvres, such as high velocity rotations.

Stange et al. (2002) proposed that the dragonfly median ocellus is adapted to resolve horizontally extended features of the world. In particular, they suggested that the horizon itself provides the most obvious indicator of body attitude during flight, and that the dragonfly ocelli may be specifically adapted to resolve this feature of the world in order to correct deviations in pitch. The results given here largely support this conclusion. The optical properties of the lens result in the widest field of view in the horizontal plane, but the highest resolution in the vertical plane. Correspondingly, the receptive fields of photoreceptors are elongated, with the long axis in the horizontal direction (present results; van Kleef et al., 2005). Additionally, the proximal limit of the rhabdom layer does not curve uniformly around the focal plane, but rather is strongly tapered in the vertical direction, with the longest and best focused rhabdoms located at the centre of the eye (Fig. 9). This arrangement results in a horizontally extended foveal streak, which in level flight is centred on the horizon. This arrangement may contribute to the one-dimensional imaging arrangement of the median ocellar L-neurons, which are staggered in azimuthal, but not elevational space along the equator of the eye (Berry et al., 2006).

However, the outputs of the ray tracing model also show that the receptive fields of photoreceptors differ markedly across the horizontal plane. This suggests that different regions of the eye may subserve different functions. The central region of the eye would be most suitable for the determination of pitch, as only horizontally extended features are well imaged in this region. More lateral regions of the eye, where resolution is good in both directions, could be utilised for other roles, such as yaw or roll detection.

5. General conclusions

Despite its simplicity, the dragonfly median ocellus possesses a number of remarkable properties. These properties include marked anisotropy in the shape, field of view and resolution of the image formed by the lens, the presence of refractive index gradients, and a remarkably high light capturing ability. The dragonfly median ocellus is deemed to be specifically adapted for limited spatial resolution, but very high temporal and contrast resolution of horizontally extended features of the world, such as the horizon.

The differences in sensitivity between locust and dragonfly ocelli, being several times higher in the latter, are presumably reflective of differences in their visual requirements. Dragonflies are extremely fast flying visual predators. As such, they need very rapid control systems with which to coordinate behaviour. Temporal resolution, and the ability to distinguish small differences in contrast—both of which require high sensitivity, are likely to be critical for dragonfly ocelli. Conversely, while locusts are active at night (which necessarily increases sensitivity requirements), they are much slower flyers. Low light conditions may be offset by longer integration times, a large degree of neural pooling, and lower requirements for contrast resolution.

Acknowledgments

This work was sponsored by the Air Force Office of Scientific Research (AFOSR), contract AOARD-03-4009. We thank Joshua van Kleef for his assistance with various aspects of ray tracing and image processing, and Prof. Mandyam Srinivasan for his ready advice in developing optical stimuli. We also thank Prof. Dan-Eric Nilsson for providing the necessary knowledge and equipment for performing interference microscopy.

References

Berry, R. P., Stange, G., Olberg, R., & van Kleef, J. (2006). The mapping of visual space by identified large second-order neurons in the dragonfly median ocellus. *Journal of Comparative Physiology A, 192*, 1105–1123.

Berry, R. P., van Kleef, J. & Stange, G. (2007a). The mapping of visual space by dragonfly lateral ocelli. *Journal of Comparative Physiology A*, in press.

Berry, R.P., Warrant, E.J. & Stange (2007b). Form vision in the insect dorsal ocelli: an anatomical and optical analysis of the locust ocelli. Vision Research, in press.

Blest, A. D., & Land, M. F. (1977). The physiological optics of *Dinopis subrufus* L. Koch: a fish-lens in a spider. *Proceedings of the Royal Society of London B, 196*, 197–222.

Chappell, R. L., & Dowling, J. E. (1972). Neural organization of the median ocellus of the dragonfly. I. intracellular electrical activity. *Journal of General Physiology, 60*, 121–147.

Chappell, R. L., Goodman, L. J., & Kirkham, J. B. (1978). Lateral ocellar nerve projections in the dragonfly brain. *Cell and Tissue Research, 190*, 99–114.

Dowling, J. E., & Chappell, R. L. (1972). Neural organization of the dragonfly ocellus. II. synaptic structure. *Journal of General Physiology, 60*, 148–165.

Fletcher, A., Murphy, T., & Young, A. (1954). Solutions of two optical problems. *Proceedings of the Royal Society of London A, 223*, 216–225.

Goodman, L. J. (1981). Organisation and physiology of the insect dorsal ocellar system. In H. Autrum (Ed.). *Handbook of sensory physiology: Comparative physiology and evolution of vision in invertebrates* (Vol. II/6C, pp. 201–286). Berlin: Springer-Verlag.

Homann, H. (1924). Zum Problem der Ocellenfunktion bei den Insekten. *Zeitschrift für Vergleichende Physiologie, 1*, 541–578.

Jagger, W. S., & Sands, P. J. (1996). A wide-angle gradient index optical model of the crystalline lens and eye of the rainbow trout. *Vision Research, 36*(17), 2623–2639.

Klingman, A., & Chappell, R. L. (1978). Feedback synaptic interaction in the dragonfly ocellar retina. *Journal of General Physiology, 71*, 157–175.

Kröger, R. H. H., Campbell, M. C. W., Munger, R., & Fernald, R. (1994). Refractive index distribution and spherical aberration in the crystalline

lens of the African cichlid fish *Haplochromis burtoni*. *Vision Research, 34*(14), 1815–1822.

Labhart, T., & Nilsson, D.-E. (1995). The dorsal eye of the dragonfly Sympetrum: specializations for prey detection against the blue sky. *Journal of Comparative Physiology A, 176*, 437–453.

Land, M. F. (1981). Optics and vision in invertebrates. In H. Autrum (Ed.). *Handbook of sensory physiology: Comparative physiology and evolution of vision in invertebrates* (Vol. II/6B, pp. 471–592). Berlin: Springer-Verlag.

Laughlin, S., & McGinness (1978). The structures of dorsal and ventral regions of a dragonfly retina. *Cell and Tissue Research, 188*, 427–447.

Meyer-Rochow, V. B. (1974). Structure and function of the larval eye of the sawfly, *Perga*. *Journal of Insect Physiology, 20*, 1565–1591.

Mobbs, P. G., Guy, R. G., Goodman, L. J., & Chappell, R. L. (1981). Relative spectral sensitivity and reverse purkinje shift in identified L neurons of the ocellar retina. *Journal of Comparative Physiology, 144*, 91–97.

Nilsson, D.-E., Gislen, L., Coates, M. M., & Garm, C. S. A. (2005). Advanced optics in a jellyfish eye. *Nature, 435*, 201–205.

Patterson, J. A., & Chappell, R. L. (1980). Intracellular responses of procion filled cells and whole nerve cobalt impregnation in the dragonfly median ocellus. *Journal of Comparative Physiology, 139*, 25–39.

Rosser, B. L. (1974). A study of the afferent pathways of the dragonfly lateral ocellus from extracellularly recorded spike discharges. *Journal of Experimental Biology, 60*, 135–160.

Ruck, P., & Edwards, G. A. (1964). The structure of the insect dorsal ocellus. I. General organization of the ocellus in dragonflies. *Journal of Morphology, 115*, 1–26.

Schuppe, H., & Hengstenberg, R. (1993). Optical properties of the ocelli of *Calliphora erythrocephala* and their role in the dorsal light response. *Journal of Comparative Physiology A, 173*, 143–149.

Simmons, P. J. (1982). The operation of connexions between photoreceptors and large second-order neurons in dragonfly ocelli. *Journal of Comparative Physiology, 149*, 389–398.

Snyder, A. W. (1977). Acuity of compound eyes: physical limitations and design. *Journal of Comparative Physiology, 116*, 161–182.

Snyder, A. W., Laughlin, S. B., & Stavenga, D. G. (1977). Information capacity of eyes. *Vision Research, 17*, 1163–1175.

Stange, G. (1981). The ocellar component of flight equilibrium control in dragonflies. *Journal of Comparative Physiology, 141*, 335–347.

Stange, G., Stowe, S., Chahl, J. S., & Massaro, A. (2002). Anisotropic imaging in the dragonfly median ocellus: a matched filter for horizon detection. *Journal of Comparative Physiology A, 188*, 455–467.

Stavenga, D. G., Bernard, D. G., Chappell, R. L., & Wilson, M. (1979). Insect pupil mechanisms. III. On the pigment migration in dragonfly ocelli. *Journal of Comparative Physiology A, 129*, 199–205.

Stone, S. L., & Chappell, R. L. (1981). Synaptic feedback onto photoreceptors in the ocellar retina. *Brain Research, 221*, 374–381.

Warrant, E. J., & McIntyre, P. D. (1991). Strategies for retinal design in arthropod eyes of low *F*-number. *Journal of Comparative Physiology A, 168*, 499–512.

Warrant, E. J., & Nilsson, D.-E. (1998). Absorption of white light in photoreceptors. *Vision Research, 38*(2), 195–207.

Williams, D. S. (1979). The physiological optics of a nocturnal semi-aquatic spider, *Dolomedes aquaticus* (Pisauridae). *Zeitschrift für Naturforschung, 34*, 463–469.

Wilson, M. (1978). The functional organisation of locust ocelli. *Journal of Comparative Physiology A, 124*, 297–316.

van Kleef, J., James, A. C., & Stange, G. (2005). A spatiotemporal white noise analysis of photoreceptor responses to UV and green light in the dragonfly median ocellus. *Journal of General Physiology, 126*, 481–497.

Zenkin, G. M., & Pigarev, I. N. (1971). Optically determined activity in the cervical nerve chain of the dragonfly. *Biofizika, 16*(2), 299–306.